



## NEW CONCEPT OF A HYBRID THERMOPLANE WITH A ROTATION BALLONETET

O. Salenko<sup>1\*</sup>, P. Pavlik<sup>1</sup>, A. Gavrushkevich<sup>1</sup>, O. Samoilenko<sup>1</sup>, O. Sulima<sup>2</sup>, V. Shchetynin<sup>2</sup><sup>1</sup>National Technical University of Ukraine "Igor Sikorsky Kyiv Polytechnic Institute"<sup>2</sup>Kremenchuk Mykhailo Ostrohradskyi National University

## ARTICLE INFO

## Article history:

Received 23 September 2021

Accepted 18 October 2021

## Keywords:

hybrid aircrafts, thermal ballonetet, composite material

## ABSTRACT

*This study gives the possibility of returning to the use of aircraft lighter than air. Hybrid aircraft can improve the performance of traditional airships. For this, a comparison was made of the main indicators of the main types of aircraft, which differ in the method of creating lift from each other. This suggests that this type of aircraft using modern materials and technologies can be re-used in modern aviation.*

*The paper considers the use of modern thermal insulation materials in the concept of an aircraft using hot air as a working fluid. It is recommended to use aerogel to store the energy of heated air. The use of aerogel as a heat-insulating material requires the study of heat exchange processes in the thermal ballonetet. Some intermediate results obtained as a result of computer simulation are presented in this paper and are descriptive.*

© 2021 Journal of the Technical University of Gabrovo. All rights reserved.

## 1. INTRODUCTION

Recently, there has been a growing interest in technology in the restoration of the use of aerostatic and hybrid aircraft. This interest is due to the efficiency of using this type of aircraft instead of conventional aircraft or helicopters. Where for economic or technical reasons their use is irrational or impossible. Which is due to the requirements of their use. The creation of new materials and their composite materials that can increase the efficiency of this type of aircraft returns the interest of investors in this topic. The main difference between these devices from the above is the aerostatic nature of the lift, which allows this device to be in the air for a significant period of time, without the use of aerodynamic surfaces.

Examples of modern devices with rigid and semi-rigid construction: "Zeppelin NT", "CargoLifter CL 160", "RA-180", "DC-H1", "Nelson", "Sky Station", "AeroCraft", "DynaLifter", "Eros ML", "Lockheed Martin P-791", "Airlander 10", "ALA-40".

## 2. COMPARISON

To perform a comparison of aircraft with different technical characteristics, it is proposed to use a coefficient that does not take into account the peculiarities of the rosy type of the aircraft type, but only its economic indicators, which determine its effectiveness.

The comparison of aircraft was performed using the following coefficients  $k_1$ ,  $k_2$  [1].

$$k_1 = \frac{m_{empt}}{m_{full}}, \quad (1)$$

$$k_2 = \frac{m_{prep}}{m_{full}}, \quad (2)$$

in these expressions  $m_{empt}$  – the mass of an empty aircraft, kg.,  $m_{full}$  – the mass of the equipped aircraft, kg.,  $m_{prep}$  – the mass of the target cargo of the aircraft, kg.,  $m_{full}$  – the weight of the equipped aircraft, kg.

The corresponding results are given in table. 1 [2], to which is also added the range of the aircraft at loading  $l_f$

and its cruising speed  $v$ ,  $\frac{km}{hour}$ .

According to the tabular data, the efficiency of aircraft by  $k_1$  and  $k_2$  with payload, range, and speed is compared. The obvious conclusion is that airships and hybrid aircraft have the best weight loss while maintaining the payload. Convertible have the worst performance. Airships and airplanes that have the highest speed have the longest range with the greatest weight return. Therefore, the problem of advanced airship construction is their quietness. At the same time, the solution to this problem is seen in the aerodynamic shape of airships and increase their speed.

## 3. RESEARCH TASK

A typical material for airship shells is a soft shell-forming material. The shape of the shell is maintained by the internal pressure of the gas. To ensure the constant shape of the soft airship, changes in the physical parameters of the environment and aerodynamic forces are taken into

\* Corresponding author. E-mail: salenko2006@gmail.com

account. Compensation for the impact of the environment is carried out by maintaining a constant pressure drop with the environment. Ballonetets are used for hybrid devices in which the bearing capacity is provided by several working gases (for example, warm air and helium, etc.). Ballonetets - soft containers located in the middle of the shell [2], the regulation of constant pressure is carried out by two valves: to release excess air and the working fluid (gas). Usually the body of the airship is made of two- or three-layer composite materials, the soft shell is made of cotton or silk fabrics, polyester materials with additional neoprene coating. Additional protection of the fabric is provided by various aluminides or coatings based on titanium oxides.

Traditionally, airships have the shape of a drop with plumage. Sometimes the load-bearing system is unified, and all power units and means of payload are performed by a separate module (unit), fig. 2.

**Table 1** Characteristics of individual aircraft

Name	$m_{full}, m.$	$m_{empt}, m.$	$m_{prep}, m.$	$k_1$	$k_2$	$l_f, км.$	$U, км/год$
<b>Aircraft</b>							
AH-225	640	250	250	0.391	0.391	7000	800
AH-124	405	180	150	0.444	0.370	4500	800
И-76	157	60	60	0.286	0.286	5000	759
B747	322	191.1	147.5	0.593	0.458	3200	855
A-380	560	276.8	83	0.494	0.148	16000	945
<b>Helicopters</b>							
Mi-26	56	28.2	20	0.504	0.357	800	265
Mi-8	11.1	7.2	2	0.649	0.180	608	250
S-65	33.3	19	14	0.571	0.420	1000	315
CH-47	22.6	10.1	2.7	0.447	0.119	370	256
<b>Convertible</b>							
V-22 Osprey	27.4	15	5.4	0.547	0.197	690	565
BA-609	7.2	4.7	1	0.653	0.139	1852	509
Bell XV-15	5.8	4.3	1	0.741	0.172	825	561
<b>Autogyro</b>							
MTO Sport.	0.495	0.241	0.254	0.487	0.513	450	185
Calidus	0.495	0.262	0.233	0.529	0.471	500	190
Cavalon	0.495	0.250	0.245	0.505	0.495	680	175
<b>Hang gliders</b>							
AEROS-2	0.472	0.21	0.26	0.445	0.551	200	90
Поиск-09	0.450	0.180	0.200	0.400	0.444	270	55
КОМЕТА	0.36	0.180	0.16	0.500	0.444	200	100
RW50	0.57	0.24	0.29	0.421	0.509	250	80
<b>Airships XX</b>							
LZ-76	63.8	31.4	32.9	0.492	0.516	7400	81
ZRS-5	182.8	109	73	0.596	0.399	10000	135
R-100	270	107	159.4	0.396	0.590	6500	131
R-101	140	116.8	25	0.834	0.179	6400	101
<b>Airships XXI</b>							
Skyship 500	4.5	1.7.	1.2	0.378	0.267	870	56
Zeppelin NT	10.6	6.1	1.9	0.575	0.179	900	120
GD-6	1.4	0.8	0.45	0.571	0.321	100	35
<b>Hybrid airships</b>							
A-N400	400	240	160	0.600	0.400	390	85
Airlander 10	20	9	10	0.450	0.500	1000	148

#### 4. MATERIAL RESEARCH

The balloon rises due to the emergence of the Archimedean force  $F_A$ ,  $H$ , which is determined by the equation:

$$F_A = g \cdot (\rho - \rho_{lift}) \cdot V, \quad (3)$$

It should be noted that hybrid airships can be heavier than air, and 60-80% of aerostatic forces are used to provide lift. The rest is provided by aerodynamic forces: engines, the shape of aircraft and other design features.

The project of the Italian company "Aerial vehicle" Nimbus EosXi in the form of a hybrid of a hang glider fig. 3. The total length of the device is 6.5 m, max. speed is 50 km/h, cruise speed 30 km/h, the duration of the aircraft in the air is 3 hours.

Thus, assume that today researchers are focusing mainly on obtaining new technical solutions for the combination of aircraft and airships, ensuring the overload of the device. Additional lifting force is obtained through the use of aerodynamic surfaces of the aircraft, the profile of the shell, similar to the profile of the wing, the use of different design of the power frame.

where  $g$  - free fall acceleration,  $\frac{m}{s^2}$ ,  $\rho$ ,  $\rho_{lift}$  - the density of the environment, and the density of the rising gas, respectively,  $\frac{kg}{m^3}$ ,  $V$  - shell volume,  $m^3$ .

At a constant volume, the lifting force increases due to the difference  $(\rho - \rho_{lift})$ , and also depends on the altitude and latitude at which the aircraft is operated.

With increasing altitude, the density and air pressure change:

$$p(h) = 4 \cdot 10^{-9} \cdot h^2 - 10^{-5} \cdot h + 1.0072, (kPa) \quad (4)$$

$$p(h) = 3 \cdot 10^{-9} \cdot h^2 - 10^{-5} \cdot h + 1.2214, (kPa) \quad (5)$$

Then  $f_{lift}$  - the specific lift of the gas can be determined by the equation  $f_{lift} = g \cdot (\rho - \rho_{lift})$ , and acquires the maximum value at  $\rho_{lift} \rightarrow 0$ . To create a lifting force and overcome the resistance forces arising from the flow around the body, and other aerodynamic surfaces  $F_{AD}$  from the generalized equation is determined:

$$F_{AD} = C_R \cdot \frac{\rho \cdot U^2}{2} \cdot S, \quad (6)$$

where  $U$  - body velocity in the air flow,  $m/s$ ,  $C_R$  - dimensionless coefficient of total aerodynamic force. With  $C_R$  determined by:

$$\bar{C}_R = \bar{C}_{lift} + \bar{C}_{drag}, \quad (7)$$

where  $C_{lift}$  - dimensionless coefficient of lifting force,  $C_{drag}$  - dimensionless coefficient of body aerodynamic resistance. These values are determined experimentally, as they depend on many parameters of the aircraft.

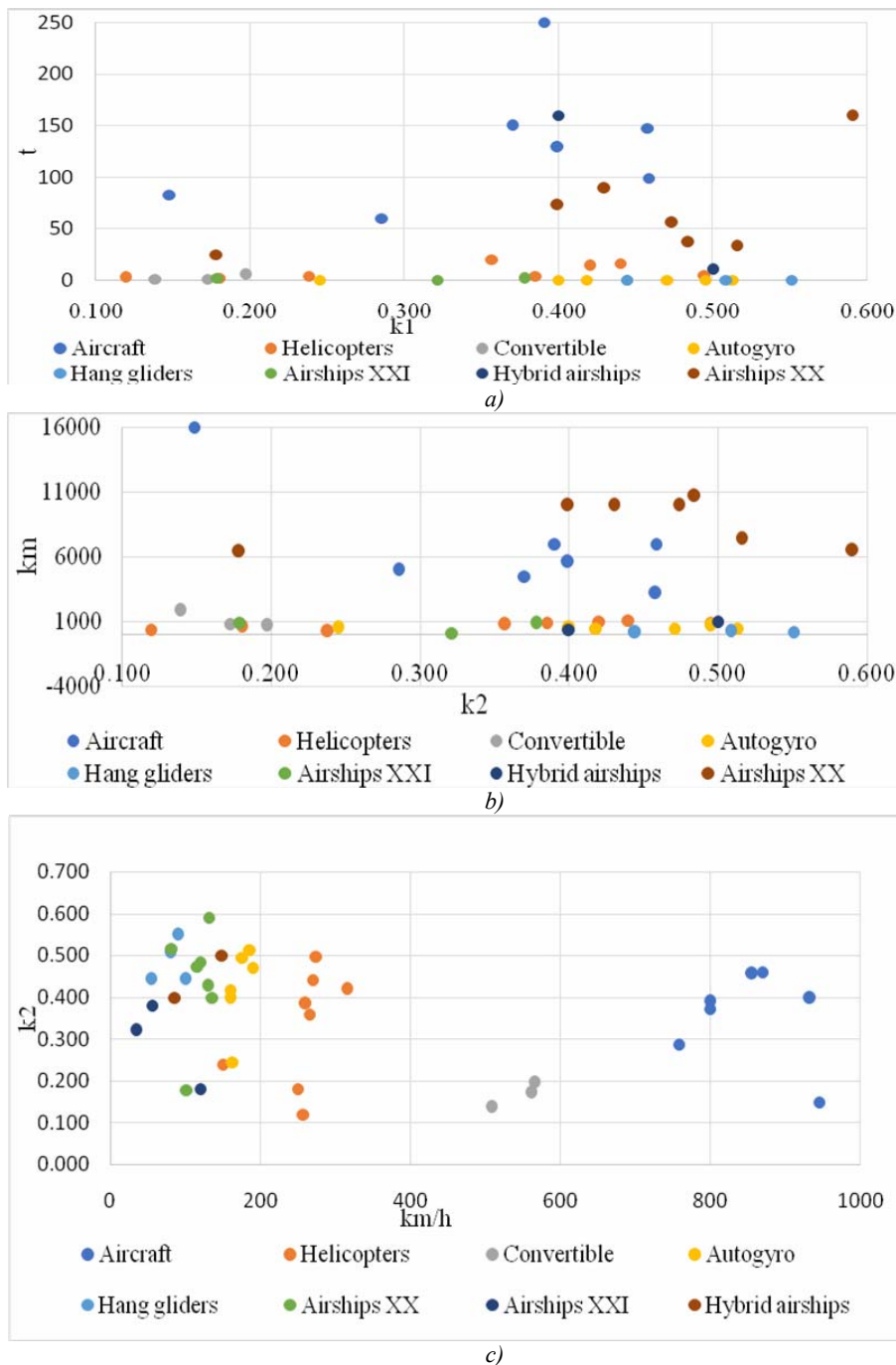


Fig. 1. Influence of mass characteristics on range, speed, loading capacity: a) coefficient  $k_1$  to  $m_{prep}$ , b) coefficient  $k_1$  to  $L$ , c) coefficient  $k_2$  to  $U$

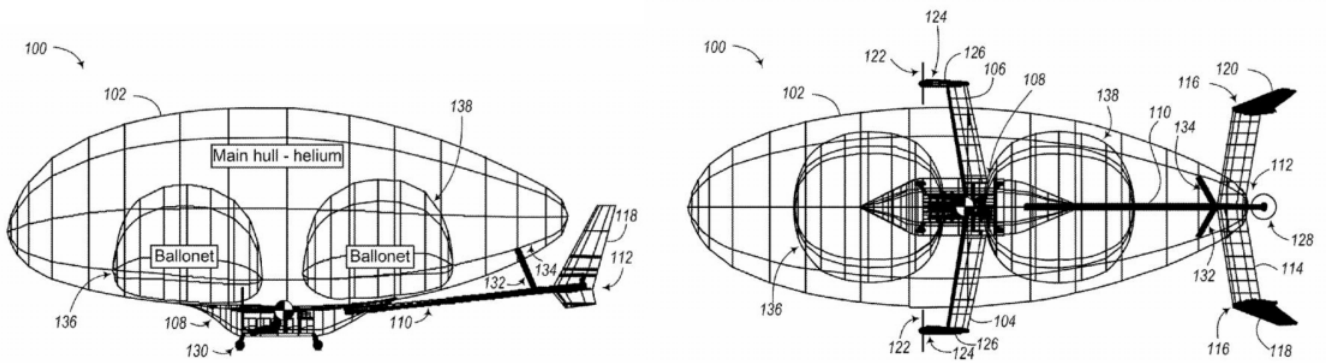


Fig. 2. PLMP Model D drone



Fig. 3. Hybrid hang glider Nimbus EosXi

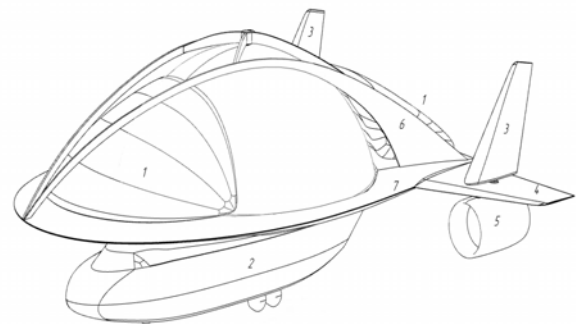


Fig. 4. Hybrid aircraft concept: 1 - light gas balloon, 2 - gondola, 3 - keel, 4 - height rudder, 5 - engine, 6 - stiffeners, 7 - rigid frame

We assume that the aircraft has a weight equal to the weight of the air it displaces, and the lifting force is provided by superheated air (heating up to 600... 700 K), the central ballonetet rotates, and additional buoyancy is provided by two balloons with light gas: H<sub>2</sub> or He. To control the pitch and roll it is proposed to use balloons filled with light helium gas ballonetets marked on fig. 4. A combination of the inertial component of the thermal balloon and the impeller 5 engines is used for control in the horizontal plane. This combination improves the speed of response to changes in the position of the aircraft in the horizontal plane.

**5. DEFINITION PARAMETERS BALLONETETS**

The weight efficiency must be equal to or higher than the following parameters adopted for the entire aircraft, namely:

$$k_2 = 0.55 \tag{8}$$

The weight of the thermal balloon includes, in addition to the weight of the shell, also the weight of the mounting, heating equipment, the weight of the rigid frame, and the control system. The equation of the sum of the masses, which determines the required lifting force to ensure the flight of a hybrid aircraft has the form:

$$m_{prep} = k_2 \cdot (m_{st} + m_{sg} + m_{ram} + m_{ap1} + m_{ap2}), kg \quad (9)$$

where  $m_{st}$  – the mass of the thermal insulation shell,  $kg$ ,  $m_{sg}$  – the mass of the gas-insulating shell,  $kg$ ,  $m_{ram}$  – the mass of the composite frame of the thermoballoon,  $kg$ ,  $m_{ap1}$  – weight of gas equipment,  $kg$ ,  $m_{ap2}$  – mass of the electric drive for rotation control,  $kg$ .

The calculation of these structural elements is performed by iterative approaches, because there are no fully defined criteria for obtaining an unambiguous result. The mass of gas and electrical equipment cannot be determined without prior calculations, and the mass of thermal insulation materials and the mass of the gas shell can be determined due to predetermined conditions. Assuming that the total mass of the thermal balloon is 1.0, the mass of the components can be determined from the proportion: thermal insulation shell  $f_1 = 0.3$ ; gas-insulating shell  $f_2 = 0.15$ ; rigid construction  $f_3 = 0.4$ ; gas equipment  $f_4 = 0.05$ ; weight of electrical equipment  $f_5 = 0.05$ .

Molar mass of the gas mixture - air is defined as the sum of the atomic masses of the elements of the gas mixture to their percentage component: 23 %  $O_2$ ; 76%  $N_2$  1% Ar:

$$Mr_{gas} = \frac{Mr(O_2) \cdot 23 + Mr(N_2) \cdot 76 + Mr(Ar) \cdot 1}{100}, \frac{kg}{mol} \quad (10)$$

The difference between the density of the environment and the density of the heated working mixture is  $f = \rho_{atm} - \rho_{gas}$ ,  $\frac{kg}{m^3}$ , and taking into account the pressure difference between the gas mixture  $\Delta p$  and the temperature of the gas mixture to the environment  $\Delta t$  the lifting force of the gas mixture in a given volume will be determined by the equation, H [3].

$$f = \rho_{atm}(h) - \frac{p_{atm}(h) + \Delta p}{(T(h) + \Delta t(h)) \cdot R} \cdot (Mr_{gas}), \frac{kg}{m^3} \quad (11)$$

where  $\rho_{atm}(h)$ ,  $T(h)$ ,  $\Delta t(h)$  – parameters that change with height.

To maintain the temperature difference in the thermal balloon, it is necessary to use the conditions of thermal balance between the heat source and the loss of the thermal balloon to the environment. To simplify the calculations, it was assumed that the large radius of the sphere  $R$  is much smaller than the thickness of the shell,  $\frac{h}{R} \ll 0.001$ . The spread of heat in the middle of the thermal balloon is due to thermal conductivity, convection and thermal radiation. The temperature distribution over the volume of the thermal balloon is determined by the temperature gradient  $\frac{\partial T}{\partial n} = gradT$ , where the law of change of temperature on normal to isothermal surfaces of distribution of heat is established.

The amount of heat transferred by thermal conductivity according to Fourier's law is determined by:

$$Q = -\lambda \cdot \frac{\partial T}{\partial n} \cdot F \cdot \tau, \quad (12)$$

where  $Q$  – the amount of heat transferred through the medium,  $J$ ,  $F$  – surface area the surface area through which heat is transferred and which receives the same amount of heat,  $m^2$ ,  $\tau$  – heat transfer time,  $\lambda$  – thermal conductivity,  $\frac{W}{m^2 \cdot K}$ .

The heat flux density can be determined by the equation

$$\bar{q} = -\lambda \cdot gradT \quad (13)$$

To describe the laws of heat exchange between the wall and the gaseous medium, we take into account the processes of convection and heat exchange. The amount of heat given off by the body through heat transfer is defined as

$$Q = \alpha \cdot (t_w - t_\infty) \cdot F, W \quad (14)$$

where  $\alpha$  – heat transfer coefficient. To take into account the forced motion of the environment, the motion of flows in the middle of the sphere, changes in temperature field, physical properties of the medium, surface characteristics used differential Fourier - Kirchhoff thermal equation which establishes the relationship between time, space and taking into account the motion of the medium:

$$\frac{\partial t}{\partial \tau} + w_x \frac{\partial t}{\partial x} + w_y \frac{\partial t}{\partial y} + w_z \frac{\partial t}{\partial z} = a \cdot \left( \frac{\partial^2 t}{\partial x^2} + \frac{\partial^2 t}{\partial y^2} + \frac{\partial^2 t}{\partial z^2} \right), \quad (15)$$

where  $a$  - coefficient of thermal conductivity,  $a = \frac{\lambda}{c \cdot \rho}$ .

This equation describes the effect of temperature increase  $\partial t$  per unit of time  $\partial \tau$  at convective heat exchange taking into account change of temperature in the directions  $\partial x$ ,  $\partial y$ ,  $\partial z$  taking into account the speed  $w_x$ ,  $w_y$ ,  $w_z$ . The convective forced and free flows that occur in the middle of the thermal balloon are determined using the Navier-Stokes equation.

$$\begin{aligned} \rho \frac{\partial w_x}{\partial \tau} + \rho \cdot \left( w_x \cdot \frac{\partial w_x}{\partial x} + w_y \cdot \frac{\partial w_x}{\partial y} + w_z \cdot \frac{\partial w_x}{\partial z} \right) &= \\ = \rho \cdot g_x - \frac{\partial p}{\partial x} + \mu \left( \frac{\partial^2 w_x}{\partial x^2} + \frac{\partial^2 w_x}{\partial y^2} + \frac{\partial^2 w_x}{\partial z^2} \right); \\ \rho \frac{\partial w_y}{\partial \tau} + \rho \cdot \left( w_x \cdot \frac{\partial w_y}{\partial x} + w_y \cdot \frac{\partial w_y}{\partial y} + w_z \cdot \frac{\partial w_y}{\partial z} \right) &= \\ = \rho \cdot g_y - \frac{\partial p}{\partial y} + \mu \left( \frac{\partial^2 w_y}{\partial x^2} + \frac{\partial^2 w_y}{\partial y^2} + \frac{\partial^2 w_y}{\partial z^2} \right); \\ \rho \frac{\partial w_z}{\partial \tau} + \rho \cdot \left( w_x \cdot \frac{\partial w_z}{\partial x} + w_y \cdot \frac{\partial w_z}{\partial y} + w_z \cdot \frac{\partial w_z}{\partial z} \right) &= \\ = \rho \cdot g_z - \frac{\partial p}{\partial z} + \mu \left( \frac{\partial^2 w_z}{\partial x^2} + \frac{\partial^2 w_z}{\partial y^2} + \frac{\partial^2 w_z}{\partial z^2} \right); \end{aligned} \quad (16)$$

To simplify the calculations, the theory of similarity of conductive, convection and radiation heat transfer, as well as taking into account mass transfer processes are used. The calculation of heat flux according to Newton's law of heat transfer is accompanied by the definition of Nusselt's criteria and Stanton's criterion:

$$Nu \equiv \frac{q_{kv}}{q_{kd}} = \frac{\alpha \cdot \Delta t}{\lambda_f \cdot \frac{\partial t}{\partial n}} = \frac{\alpha \cdot R_0}{\lambda_f}, S_t = \frac{\alpha}{\rho \cdot C_p \cdot v_0}, \quad (17)$$

There  $q_{kv}$  - heat flux density of convective heat transfer,  $q_{kd}$  - density of conductive heat transfer,  $R_0$  - characteristic size in the system of convective heat transfer,  $\rho$  - medium density,  $C_p$  - heat capacity of the environment,  $v_0$  - flow rate,  $\frac{m}{s}$ .

Determination of the maximum heat flux density through the walls is determined under the conditions of achieving the appropriate constraints for heat flux: no convection exchange, convection from the atmosphere and the ballonet, neglect of the thermal conductivity of the film, the flux density is evenly distributed throughout the volume. The heat flux density according to Newton's equation is determined as follows:

$$q_f = \frac{\lambda_0}{h} \cdot \left( 1 + k \cdot \frac{t_g + t_a}{2} \right) \cdot (t_g - t_a), \frac{W}{m^2} \quad (18)$$

where  $\lambda_0 = 13.4 \frac{mW}{m \cdot K}$  - thermal conductivity,  $h$  - wall thickness,  $m$ .

The shell of the thermal balloon consists of a thermal layer and a gas insulating layer. These materials differ in their structure and have different mechanical properties. The heat-insulating shell has orthotropic properties, and the gas-insulating anisotropic one. Between these data shells to simplify the calculations will be taken as tightly glued over the entire area. The thickness of the shell is several orders of magnitude less than the overall dimensions of the entire structure, so in the calculations of the transverse moments that occur in the shell is neglected.

Considering the forces acting on the thermal balloon, it is necessary to pay attention to the calculation of the shell for strength at the attachment points and determine the internal additional pressure to maintain the shape of the shell, to determine the thickness of the shell. To calculate

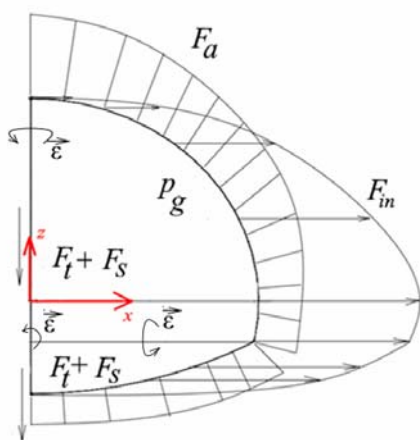


Fig. 5. Loads acting on the shell

the shell, it is necessary to establish the relationship between stresses.

where  $F_t$  - the weight of the insulating layer,  $H$ .  $F_s$  - weight of gas insulating shell,  $H$ .  $p_g$  - internal excess pressure that occurs in the shell,  $Pa$ .  $F_{in}$  - force of inertia acting on the shell due to rotation,  $H$ .  $F_a$  - the power of Archimedes,  $H$ .  $\epsilon$  - angular acceleration of the shell. To determine the stresses, the stress theory of thin shells was considered. The radius of curvature of the shell  $R$  is the same in both the medial and circumferential directions. Because the ratio of the film thickness  $\delta$  to  $R$  are in the range  $10^{-5} \leq \frac{\delta}{R} \leq 10^{-2}$ .

This condition allows the use of Lava-Kirchhoff hypotheses in the calculation of thin shells [4]:

- direct normal to the middle surface in the process of deformation is not curved, but remains perpendicular to the middle surface,
- the length of the normal to the middle surface, does not change during deformation,
- the thickness of the plate does not change during deformation.

Lamé coefficients are determined for geometric reasons fig. 6.

For a spherical coordinate system at  $\beta = \varphi$  and  $\alpha = \nu$  as result:

$$\begin{aligned} h_1 &= R \\ h_2 &= R \cdot \sin \alpha \end{aligned} \quad (19)$$

where  $R$  - the distance from the pole to the studied single element.

The equilibrium equation for the unit area of a thin shell under the action of the forces of the rejected part of the shell and the external forces acting on the shell. In fig. 7 shows the forces arising on the elementary middle surface of the shell.

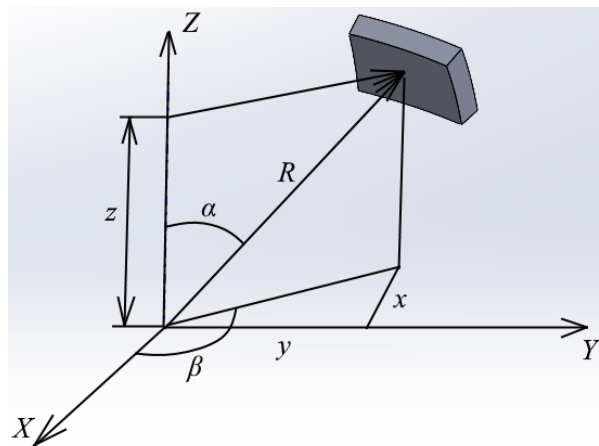


Fig. 6. Determination of Lamé coefficients

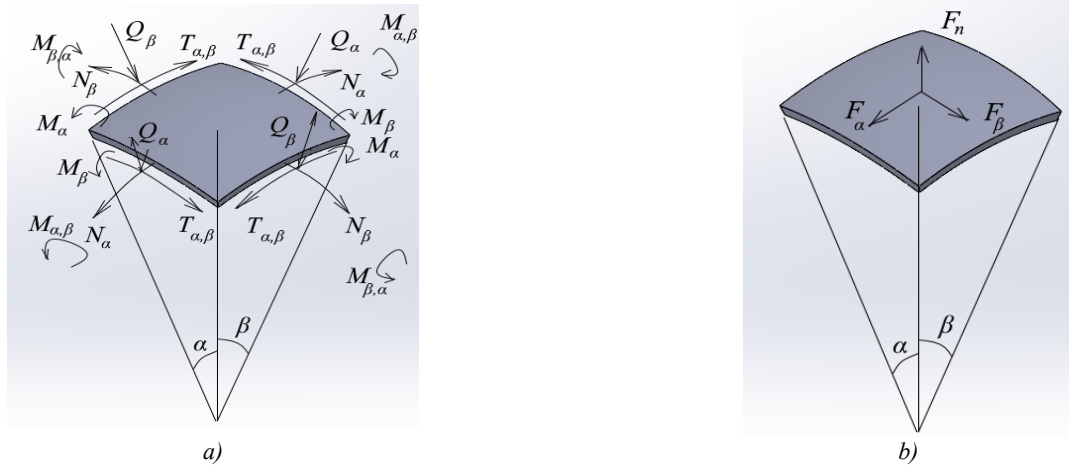


Fig. 7. Loads acting on the elementary site of the middle surface: a) from discarded items, б) external loads

The system of balance of efforts after the membership differentiation will look like [5].

$$\begin{aligned} \frac{1}{h_1 \cdot h_2} \left( \frac{\partial(h_1 \cdot N_\alpha)}{\partial \alpha} + \frac{\partial(h_1 \cdot T_{\alpha\beta})}{\partial \beta} + T_{\alpha\beta} \frac{\partial h_1}{\partial \beta} - N_\beta \frac{\partial h_2}{\partial \alpha} \right) + \frac{Q_\alpha}{R} + F_\alpha &= 0 \\ \frac{1}{h_1 \cdot h_2} \left( \frac{\partial(h_2 \cdot T_{\alpha\beta})}{\partial \alpha} + \frac{\partial(h_1 \cdot N_\beta)}{\partial \beta} + T_{\alpha\beta} \frac{\partial h_2}{\partial \alpha} - N_\alpha \frac{\partial h_1}{\partial \beta} \right) + \frac{Q_\beta}{R} + F_\beta &= 0 \quad (20) \\ \frac{1}{h_1 \cdot h_2} \left( \frac{\partial(Q_\alpha \cdot h_2)}{\partial \alpha} + \frac{\partial(Q_\beta \cdot h_1)}{\partial \beta} \right) - \frac{N_\alpha}{R} - \frac{N_\beta}{R} + F_n &= 0 \end{aligned}$$

The equilibrium system of moments acting on the shell is determined from the formulas [4].

$$\begin{aligned} \frac{1}{h_1 \cdot h_2} \left( \frac{\partial(h_2 \cdot M_{\alpha\beta})}{\partial \alpha} + \frac{\partial(h_1 \cdot M_\beta)}{\partial \beta} - M_\alpha \frac{\partial h_1}{\partial \beta} + M_{\alpha\beta} \frac{\partial h_2}{\partial \alpha} \right) &= Q_\beta \quad (21) \\ \frac{1}{h_1 \cdot h_2} \left( \frac{\partial(h_2 \cdot M_\alpha)}{\partial \alpha} + \frac{\partial(h_1 \cdot M_{\alpha\beta})}{\partial \beta} + M_{\alpha\beta} \frac{\partial h_1}{\partial \beta} - M_\beta \frac{\partial h_2}{\partial \alpha} \right) &= Q_\alpha \end{aligned}$$

After simplification, the equilibrium expressions of the shell element are obtained

$$\begin{aligned} \frac{1}{h_1 \cdot h_2} \left( \frac{\partial(h_1 \cdot N_\alpha)}{\partial \alpha} + \frac{\partial(h_1 \cdot T_{\alpha\beta})}{\partial \beta} + T_{\alpha\beta} \frac{\partial h_1}{\partial \beta} - N_\beta \frac{\partial h_2}{\partial \alpha} \right) + F_\alpha &= 0 \\ \frac{1}{h_1 \cdot h_2} \left( \frac{\partial(h_2 \cdot T_{\alpha\beta})}{\partial \alpha} + \frac{\partial(h_1 \cdot N_\beta)}{\partial \beta} + T_{\alpha\beta} \frac{\partial h_2}{\partial \alpha} - N_\alpha \frac{\partial h_1}{\partial \beta} \right) + F_\beta &= 0 \\ \frac{N_\alpha}{R} + \frac{N_\beta}{R} &= 0 \end{aligned}$$

Since the use of a two-layer shell is assumed, according to Hooke's law, the meridional stresses and circumferential stresses will be determined by (19) in each individual layer denoted by *i*. And the tangential stresses in a separate layer will be determined as follows:

$$\begin{aligned} \sigma_{1i} &= \frac{E_{1i}}{1 - \mu_{1i} \cdot \mu_{2i}} (\varepsilon_{1i} + \mu_{2i} \cdot \varepsilon_{2i}) \\ \sigma_{2i} &= \frac{E_{2i}}{1 - \mu_{1i} \cdot \mu_{2i}} (\varepsilon_{2i} + \mu_{1i} \cdot \varepsilon_{1i}) \quad (22) \\ \tau_{12i} &= G_i \cdot \gamma_{12i} \end{aligned}$$

**6. CAE MODELING AND DISSCUSSION**

A diffuser burner with pre-injection of air is used for a stable combustion process. This type of burner provides an intensive combustion chamber with complete completion of the combustion process. The scheme of a direct-flow diffusion heater with a central gas supply is shown in fig. 8. Working gas - hydrogen (H<sub>2</sub>) [5], [6].

Hydrogen combustion occurs completely, the equivalent ratio of fuel to oxidant  $\varphi = 1$ . The heat of combustion of fuel is considered to be a partially adiabatic problem, the heat of combustion is not removed by the walls of the heater, but is removed through the outlet. To simplify the calculations, modeling of the chemical oxidation reaction with water without taking into account other reactions is used. The reaction occurs at high speed. Extreme cases are considered.

In the first case, the parameters of the gas equipment and partial input parameters during stationary operation of the burner were determined.

At the inlet of the nozzle, the hydrogen saturation of the gas mixture is 100%, and at the inlet of the air in the diffuser 23%. The distribution of temperature and flow rate is shown in fig. 9.

The main sources of heat loss are the wall and outlets. The total power consumption through the wall is approximately 715W. Through the outlets, the loss is 371 W. Ignoring other costs, the power of the source is 1500 W.

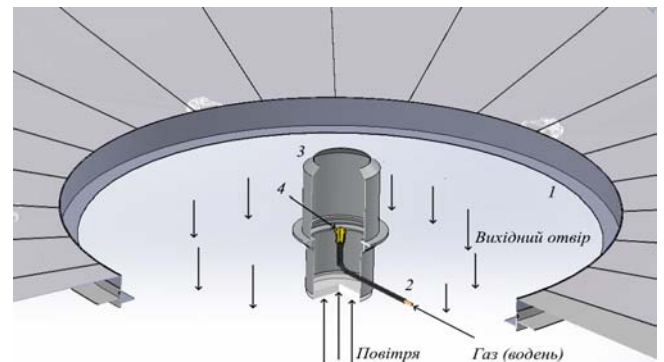


Fig. 8. Scheme of a direct-flow diffuser with a central gas supply

The behavior of the shell itself was assessed using Solidworks Simulations. The following calculation cases are accepted: stationary state, shell rotation, motion with rotation. The forces acting on the shell at these loads in the calculated cases are given in Fig. 10.

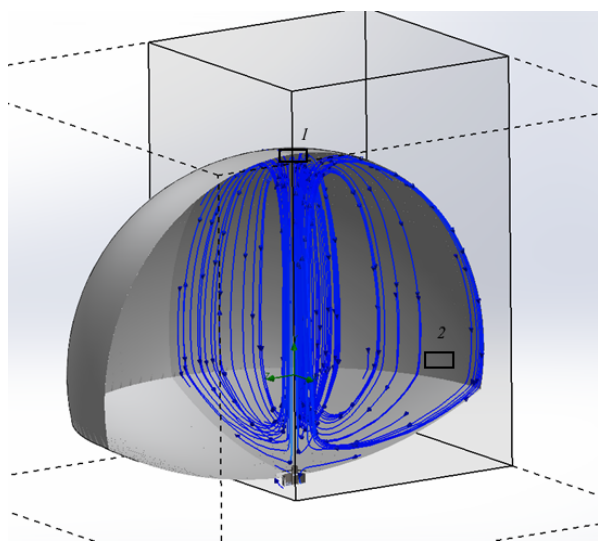
Where  $\varepsilon$ , angular velocity  $\omega$ , linear acceleration  $a$ . The shell state parameters are calculated from the equations given above. The gas shell is considered as a spherical shell. Thermal insulation is taken into account by the distributed mass on the shell. The scheme of fastening of a cover is shown in fig. 11.

During the calculations, the distribution of stresses and strains in the shell, shown in fig. 12; the simulation conditions are given in table 2 on the critical pressure (30 kPa) and rotation speed (15,2 m/s) according the angular velocity is maximum  $0,5 \text{ s}^{-1}$ .

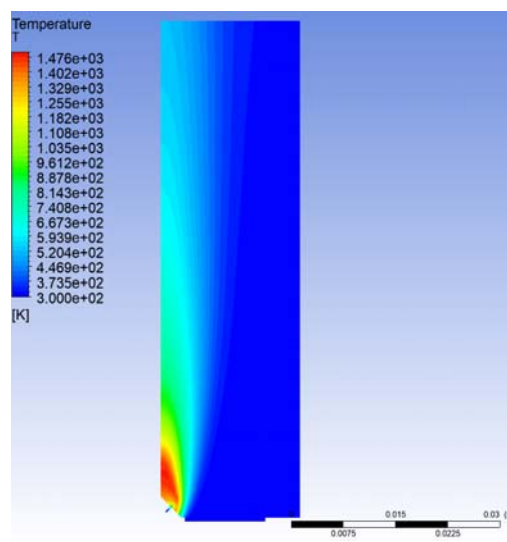
Therefore, it becomes obvious that the soft shell is able to retain its shape at an overpressure of about  $19,0 \text{ kPa}$  when rotating around the vertical axis at a speed of  $0,5 \text{ s}^{-1}$ , which allows the aircraft to have a stabilized position when performing aerobatic tasks, and not spend extra energy to ensure a given position of the device. Having a heater with a capacity of  $1.5 \text{ kW}$ , and using as a thermal

balloon asymmetric ball with a diameter of  $10.0 \text{ m}$ , as well as a soft shell with a heat insulator in the form of an airtel,  $2.0 \text{ mm}$  thick, [7] we obtain a lifting force for an overloaded device at  $6.9 \dots 7.1 \text{ kg}$ .

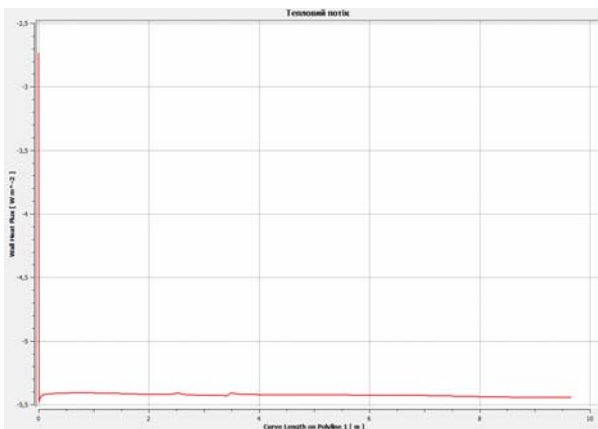
This value at certain volumes of the thermal balloon is not enough, and that is why it is proposed to use He as an additional gas, which for these conditions can provide neutral buoyancy of the device, i.e. equalization of its mass (payload) to the mass of displaced air. At the expense of a thermoballoon the vertical raising and lowering of the device will be carried out.



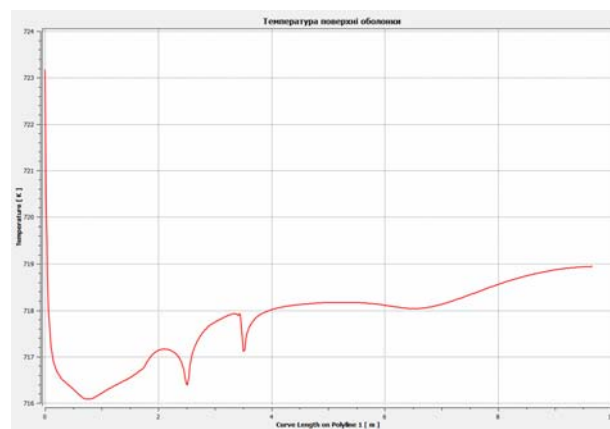
a) convection in the ballonnet



b) temperature distribution field from the burner



c) heat flow through the wall



d) temperature distribution along the wall

Fig. 9. Thermal processes

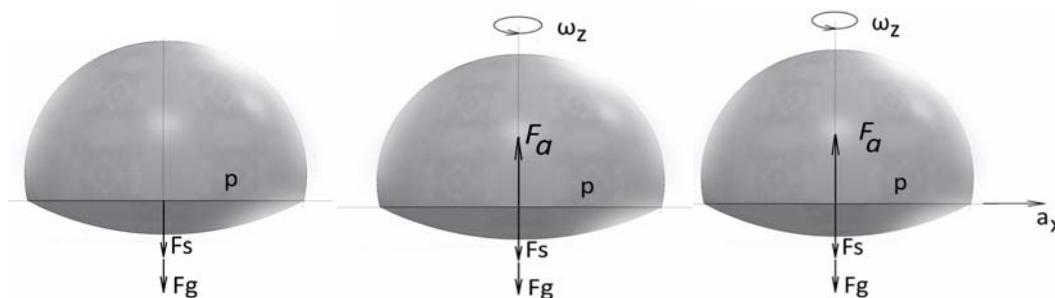


Fig. 10. Estimated cases



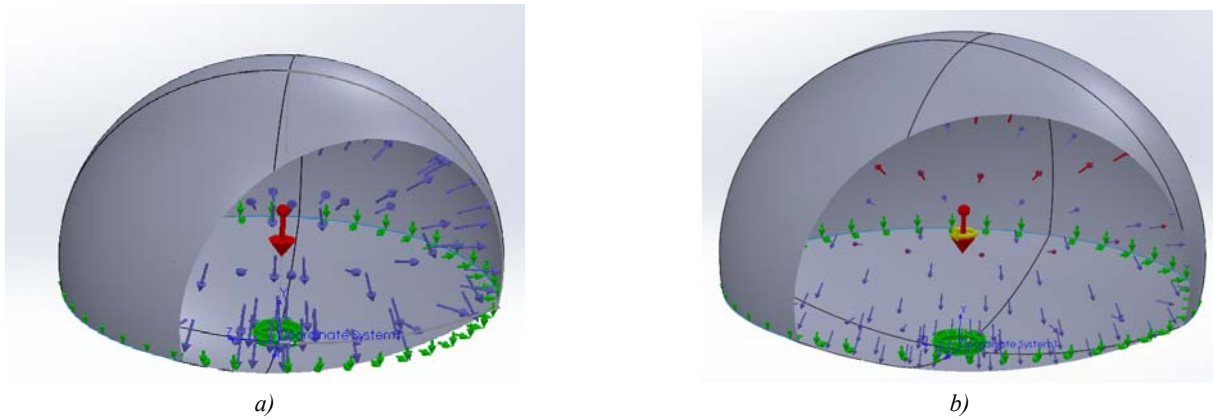


Fig. 11. Efforts are applied to the shell

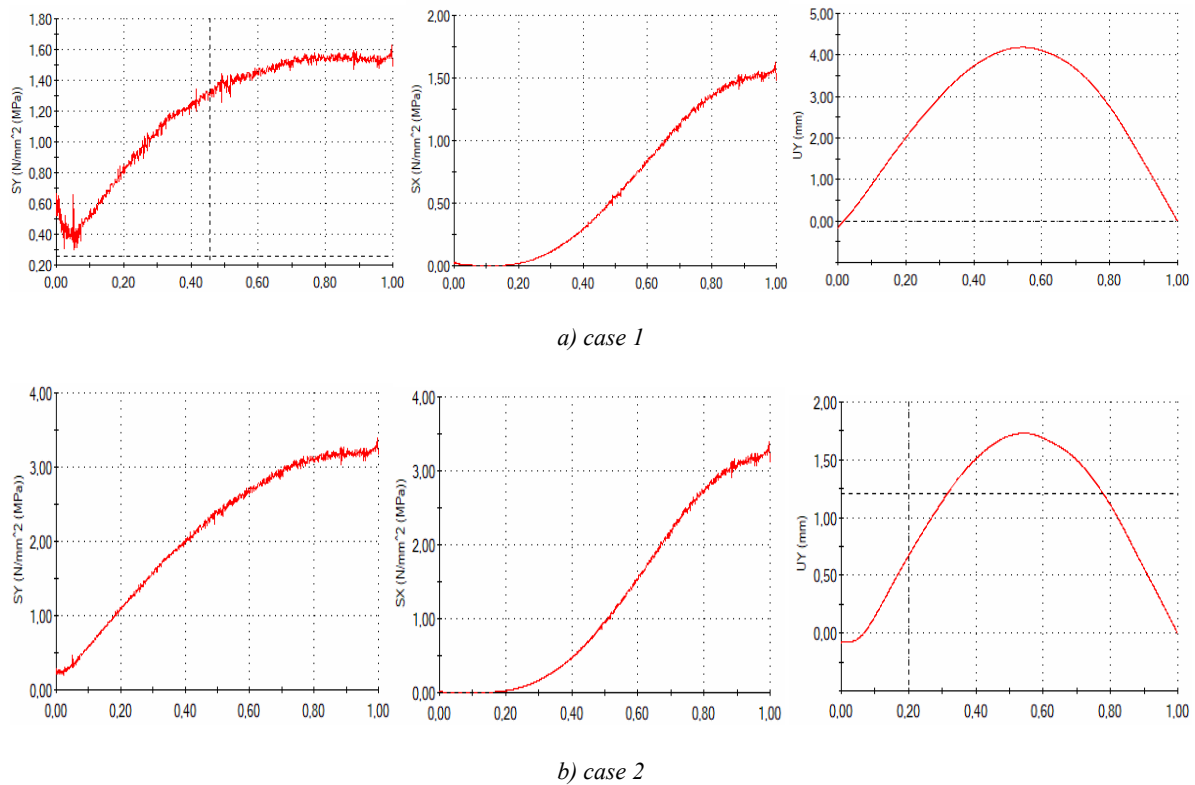


Fig.12. The stresses in the shell are meridional, the circumferential stresses, MPa and displacements are generalized, mm

Table 2 The researched parameters

Parameters	Case 1	Case 2
The thickness of the film, mm	1.0	1.5
The pressure is maximum, kPa	19.0	8
The pressure is minimal, kPa	1.8	0
The angular velocity is maximum, $s^{-1} \frac{rad}{s}$	0	0.5 (3,5)
Angular velocity is minimal, $s^{-1}$	0	0

Thus, the concept of creating lighter devices from the air, in which buoyancy in the atmosphere is provided by light gas, and the rise and fall of the device - thanks to the thermal balloon, is energy efficient and rational, because the vertical movement of the device does not need to release or replenish valuable light gas. with reliable compaction of balloons and virtually no loss of light gas control due to the thermocouple should be tied to the load

capacity of the aircraft, and the thermal performance of the burners will determine both the flight range and lifting height of the aircraft.

Further research should be aimed at identifying a rational speed of rotation of the balloon, as well as to establish the ratio of the volume of the chambers of light gas and hot air, based on the condition of maintaining heat in the balloon during the flight. As the thermal balloon shell

is exposed to heat and pressure, lightweight frame structures must be used to preserve its shape.

## CONCLUSION

As a result of the study, the theoretical possibility of using aerogel as a thermal insulation material was established. The calculation of the thermal balloon for strength and stability conditions using the theory of thin-walled shells is substantiated. From this formula, the minimum and maximum pressure drop was obtained to maintain its shape.

The basic laws of temperature distribution in the middle of the balloon are determined, taking into account the heat exchange of processes with the environment. The temperature distribution inside the thermal balloon is determined.

Using the values found, the possibility of using modern hybrid aircraft in modern aviation was substantiated.

## REFERENCES

- [1] Busemeyer K.L., Hot Air Airships. Airship Technology, Cambridge: Cambridge University Press, 2012
- [2] Kirilin A.N., Airships, Moscow: MAI-PRINT Publishing House, 2013
- [3] Busemeyer K.L., Hot Air Airships. Airship Technology, Cambridge: Cambridge University Press, 2012
- [4] Stockbridge C.M., Stability and Control of Unconventional Airships, Design and Experimental Investigations, MS Thesis, Mechanical and Aeronautical Engineering Department, Clarkson University, Potsdam NY, 2012
- [5] Ardema M.R., Airship, Access Science, McGraw-Hill Companies, 2008, access: <http://www.accessscience.com>
- [6] Sokolov E.Ya. Teplofikatsiya i teplovye seti [District heating and heat network]. Moscow, MEI Publ., 2001. 472 p.
- [7] Salenko O.F., Pavlyk P.M., Doslidzhennya konstruktivnoy ta materialiv dlya novykh prohresyvnnykh aparativ lehshykh povitrya. – Forum Ingheneriv-mechanikiv (2019) 216-223